Tellus
SERIES A
DYNAMIC
METEOROLOGY
AND OCEANOGRAPHY
PUBLISHED BY THE INTERNATIONAL METEOROLOGICAL INSTITUTE IN STOCKHOLM

Tellus (2011), 63A, 312–323

TELLUS

Sea-ice anomalies in the Sea of Okhotsk and the relationship with storm tracks in the Northern Hemisphere during winter

By MICHEL D. S. MESQUITA[1,2,3]*, KEVIN I. HODGES[4], DAVID E. ATKINSON[3] and JÜRGEN BADER[2,5], [1]*Uni Bjerknes Centre, Allegaten 55, NO-5007, Bergen, Norway*; [2]*Bjerknes Centre for Climate Research, Allegaten 55, NO-5007, Bergen, Norway*; [3]*Department of Atmospheric Sciences, University of Alaska Fairbanks, International Arctic Research Center, 930 Koyukuk Drive, Fairbanks, AK 99775, USA*; [4]*National Centre for Earth Observation, University of Reading, Whiteknights, PO Box 238, Reading, RG6 6AL, UK*; [5]*University of Bergen, Geophysical Institute, Allegaten 70, NO-5007, Bergen, Norway*

(Manuscript received 30 November 2009; in final form 20 August 2010)

ABSTRACT

Previous studies have shown that sea-ice in the Sea of Okhotsk can be affected by local storms; in turn, the resultant sea-ice changes can affect the downstream development of storm tracks in the Pacific and possibly dampen a pre-existing North Atlantic Oscillation (NAO) signal in late winter. In this paper, a storm tracking algorithm was applied to the six hourly horizontal winds from the National Centers for Environmental Prediction (NCEP) reanalysis data from 1978(9) to 2007 and output from the atmospheric general circulation model (AGCM) ECHAM5 forced by sea-ice anomalies in the Sea of Okhotsk. The life cycle response of storms to sea-ice anomalies is investigated using various aspects of storm activity—cyclone genesis, lysis, intensity and track density. Results show that, for enhanced positive sea-ice concentrations in the Sea of Okhotsk, there is a decrease in secondary cyclogenesis, a westward shift in cyclolysis and changes in the subtropical jet are seen in the North Pacific. In the Atlantic, a pattern resembling the negative phase of the NAO is observed. This pattern is confirmed by the AGCM ECHAM5 experiments driven with above normal sea-ice anomalies in the Sea of Okhotsk.

1. Introduction

Yamamoto et al. (2006) briefly summarize the 'chicken and egg' discussions that now surround the linkage between the atmosphere and sea ice—what drives what. The first-order view suggests that it is the atmosphere that drives the sea-ice state, as discussed by, for example, Rogers and van Loon (1979) or Partington et al. (2003). In the last 20 yr, climate studies have reliably indicated that sea ice does not only passively respond to atmospheric drivers but can in fact influence the atmosphere (e.g. Honda et al. 1999). Alexander et al. (2004) explore this theme in more detail, reviewing previous work that demonstrates how the sea ice impacts the local low levels of the atmosphere on a fairly short-term basis (on the order of weeks), and also upper levels of the atmosphere with varying temporal lags. They also point to various hypotheses that take the temporal lag process as far as linking sea ice to decadal oscillations.

Several other studies show that sea-ice concentration has an effect on the atmosphere. For example, using a series of General Circulation Model (GCM) experiments in which Southern Hemisphere sea-ice concentration was progressively altered from 5% to 100% open lead, Simmonds and Budd (1991) suggest that Antarctic sea ice influences the Southern Oscillation. In the Northern Hemisphere, other modelling studies have shown that sea ice can have an impact on the North Atlantic Oscillation (Deser et al., 2004; Magnusdottir et al., 2004; Seierstad and Bader, 2009).

One mechanism by which sea ice and the atmosphere are linked is via cyclones/storms. Storms can have a demonstrable and almost immediate effect on sea-ice concentration and extent. Overland and Pease (1982) in fact suggest that sea-ice extent is heavily dependent on the action of storms: primarily, via their preferred pathway in a given season, and less so, via the total number of storms. The mechanism they present invokes advection as the means by which storms exert their influence: heavy ice years in the Bering Sea result from a more southerly position of the storm tracks there, advecting cold air from the Alaskan and northwest North American interior regions; light ice years

*Corresponding author.
e-mail: michel.mesquita@uni.no
DOI: 10.1111/j.1600-0870.2010.00483.x

occur when a larger number of storms track along the west side of the Bering Sea, advecting warm air northwards.

The Sea of Okhotsk ('SOK' hereafter) is the southern most marginal sea that exhibits an annual ice cover of sufficient size to exert an influence on the atmosphere. This ice cover is influenced by the action of storm systems, for example, in the manner of Overland and Pease (1982), but the resultant anomalies in turn can affect the downstream development of storm tracks (Honda et al., 1999). This two-way interaction process alters local albedo and fluxes of heat and temperature, with demonstrable broader implications for Northern Hemisphere circulation. Sea ice acts as a lid affecting the fluxes of mass, heat and momentum. It reduces the solar absorption at the surface and it serves as an insulator.

A few studies have considered the influence of sea-ice changes over the SOK (Murray and Simmonds, 1995; Honda et al., 1999; Alexander et al., 2004; Yamamoto et al., 2006), either exclusively or as part of a broader study of the Northern Hemisphere, but mostly from a modelling perspective. None have considered the low-frequency variability changes due to the sea-ice conditions in the SOK based on objective tracking of individual storm tracks. Do the changes of sea-ice configuration in the SOK really matter for storms?

Using a combination of observed SOK sea-ice extent and concentrations, data from reanalyses, and atmospheric general circulation model (AGCM) integrations with idealized SOK sea-ice concentration, this study aims to build upon previous studies to explore, in greater detail, the following points:

(1) establish the changes in storm tracks related to winter sea-ice anomalies in the SOK. This is based on an index of sea-ice anomalies and using objective feature tracking of extratropical cyclones;

(2) consider whether the SOK sea-ice changes only affect the downstream development of storm tracks in the Pacific, as in Honda et al. (1999), or if there are significant changes in the Atlantic storm tracks as well;

(3) determine the storm track changes due to prescribed sea-ice concentration in the SOK region using AGCM simulations.

2. Methods and data sets

Monthly sea-ice extent (in km^2) and concentration data for the SOK were obtained from the National Snow and Ice Data Center (NSIDC) for the period 1978–2007. This data set is generated from brightness temperatures derived from satellites, with radiances resolved at a grid cell size of 25 by 25 km (Cavalieri et al., 2008). Two indices were created by a monthly standardization of the extent and concentration data sets (for December, January and February). These will be used to make composites of cyclone activity.

2.1. Storm tracking

Storms were tracked using the algorithm developed by Hodges (1994, 1995, 1996, 1999), which has yielded useful results in previous studies (e.g. Hoskins and Hodges, 2002; Mesquita et al., 2010). The tracking variable used in the algorithm was the relative vorticity at the 250 hPa and the 850 hPa levels. This variable is chosen because it is less influenced by the background flow. It also focus on the smaller-spatial-scale end of the synoptic range so that many more systems are generally identified, as compared to mean sea level pressure (MSLP), which focuses on the large-scale end (Hodges et al., 2003). Relative vorticity is also related to the winds since it is defined as the vertical component of the curl of the relative velocity. Once cyclones are identified as maxima in the relative vorticity fields, the correspondence between the feature points in consecutive time steps is determined by the minimization of a cost function (see Hodges, 1995 for more details). The resultant storm data were filtered to retain only those systems that last longer than 2 d and travel further than 1000 km, so that only mobile systems are considered.

The relevant fields for the tracking were obtained from the NCEP/NCAR global reanalysis (R1) (Kalnay et al., 1996; Kistler et al., 2001) from 1978/1979–2007 provided by NOAA/NWS/NCEP (NCEP Reanalysis data provided by the NOAA/OAR/ESRL PSD, Boulder, Colorado, USA, from their Web site at http://www.cdc.noaa.gov/). The tracking requires six hourly vorticity, which is obtained from the horizontal winds. The period considered for the tracking analysis applied to the reanalysis is chosen to correspond with the SOK indices.

The statistics of the storm track patterns for the positive and negative anomalies of the SOK indices were determined based on the compositing method in Bengtsson et al. (2006). These tracking statistics are calculated using spherical kernel estimators, described in Hodges (1996), and the influence of the SOK sea-ice anomaly indices is introduced into the statistics by introducing additional weights computed from the index. The benefit of using this approach is grounded in methodological utility rather than physical considerations: it allows more of the data to be used as opposed to applying a straightforward threshold. This can be important if the data period is relatively short. The storm track response to SOK sea-ice anomalies was calculated by producing composite statistics for the positive and negative anomalies using the SOK indices for the winter (DJF) period from the NCEP reanalysis data for 1978–2007.

The significance for the storm track difference plots is computed using a permutation Monte Carlo approach (see Hodges, 2008 for details) from which p-values are obtained. A value of $p \leq 0.05$ (95%) is chosen as the critical value to indicate rejection of the null hypothesis. This approach has been applied in other storm track studies, for example, Bengtsson et al. (2006) and Woollings et al. (2010).

2.2. Model and experiments

The atmospheric model used in this study is the AGCM ECHAM5 (Roeckner et al., 2006), described in full detail in a technical report (Roeckner et al., 2003). This model has

previously been used for sea-ice experiments (Seierstad and Bader, 2009) and the analysis of storm tracks (Bengtsson et al., 2006).

The atmospheric model is run at T63 (∼1.875° × 1.85°) horizontal resolution with 31 vertical levels. Two sets of ensembles, each consisting of 30 experiments, were conducted. Each experiment member only differs in the initial conditions, which were chosen from a separate control integration.

For computational economy, each experiment was run for 4 months starting from first of December until the end of March. The ECHAM5 model is forced by the climatological annual cycle of global sea surface temperatures and sea-ice concentrations except in the SOK. In the SOK, the sea-ice concentrations have been set to zero for one ensemble and to 100% for the other. All other external forcings (e.g. greenhouse gases, solar radiation) are the same for all integrations. The only difference between the two ensembles is the sea-ice concentration in the SOK.

3. Results

3.1. The SOK sea-ice variability

The observed winter SOK sea-ice concentration varies from very low in December to high in February (Fig. 1a). Most of the variability is in January and February and the average winter sea-ice concentration is similar to that in January. Figure 1b shows the SOK concentration index ('SOKc', hereafter). The sea-ice extent and concentration in the SOK are highly correlated (not shown), and even though both indices were tested in this study, only results using SOKc were retained for further analysis. On average, the SOKc index was positive from 1979 to 1987 (except 1981 and 1984), from 1993 to 1995 and from about 1999 to 2003 (except 2000) and it was negative otherwise. In spite of this and the slight decline in the early 1980s, no particular long-term trend is evident when considering the entire timeseries. The year 1996 was the record minimum sea-ice extent in the SOK for the months of January and December, in agreement with Toyota et al. (1999) page 119, who observed that 'Since the data became available in 1971, the sea-ice extent in the Okhotsk Sea in 1996 was record-breakingly small. . .'.

3.2. Extratropical storm tracks and the SOKc index

Figure 2 shows the difference between the positive and negative composites of the SOK concentration index (SOKc+ minus SOKc–) for four track variables: (1) genesis density (*gdens*)—density of track starting points per one million square kilometers per season [$(10^6$ km^2 season$)^{-1}$]; (2) track density (*tdens*)—number of storm tracks through a region per $(10^6$ km^2 season$)^{-1}$; (3) lysis density (*ldens*)—density of ending track points per (10^6

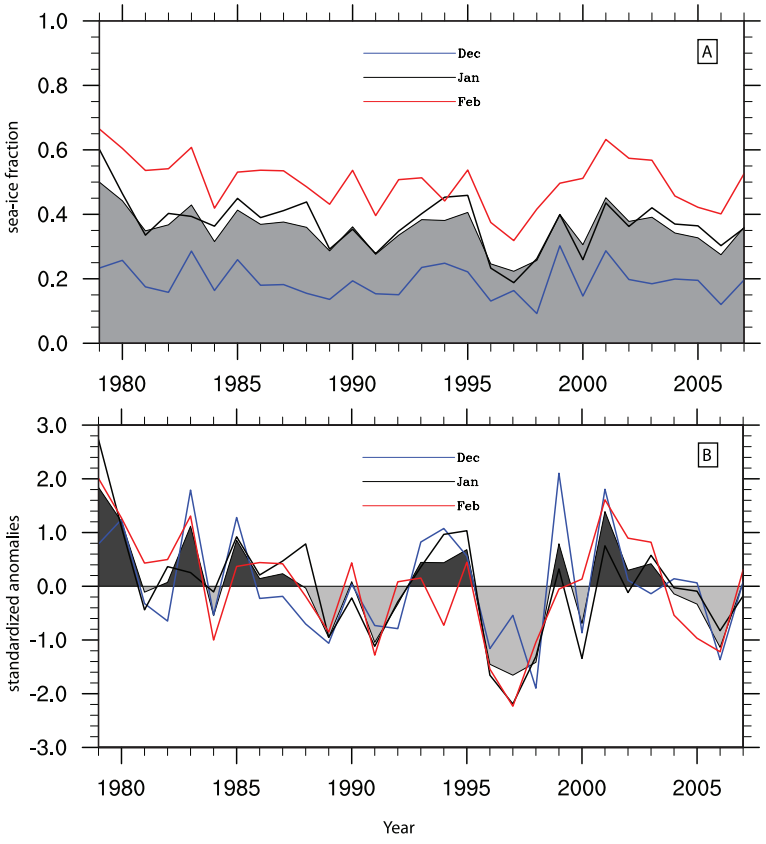

Fig. 1. (a) Sea-ice fraction in the Sea of Okhotsk (SOK) for December, January and February from 1978(9) to 2007. Shading in the background represents the average DJF sea-ice concentration. (b) SOKc standardized anomalies for December, January and February. Shading represents the average DJF SOKc.

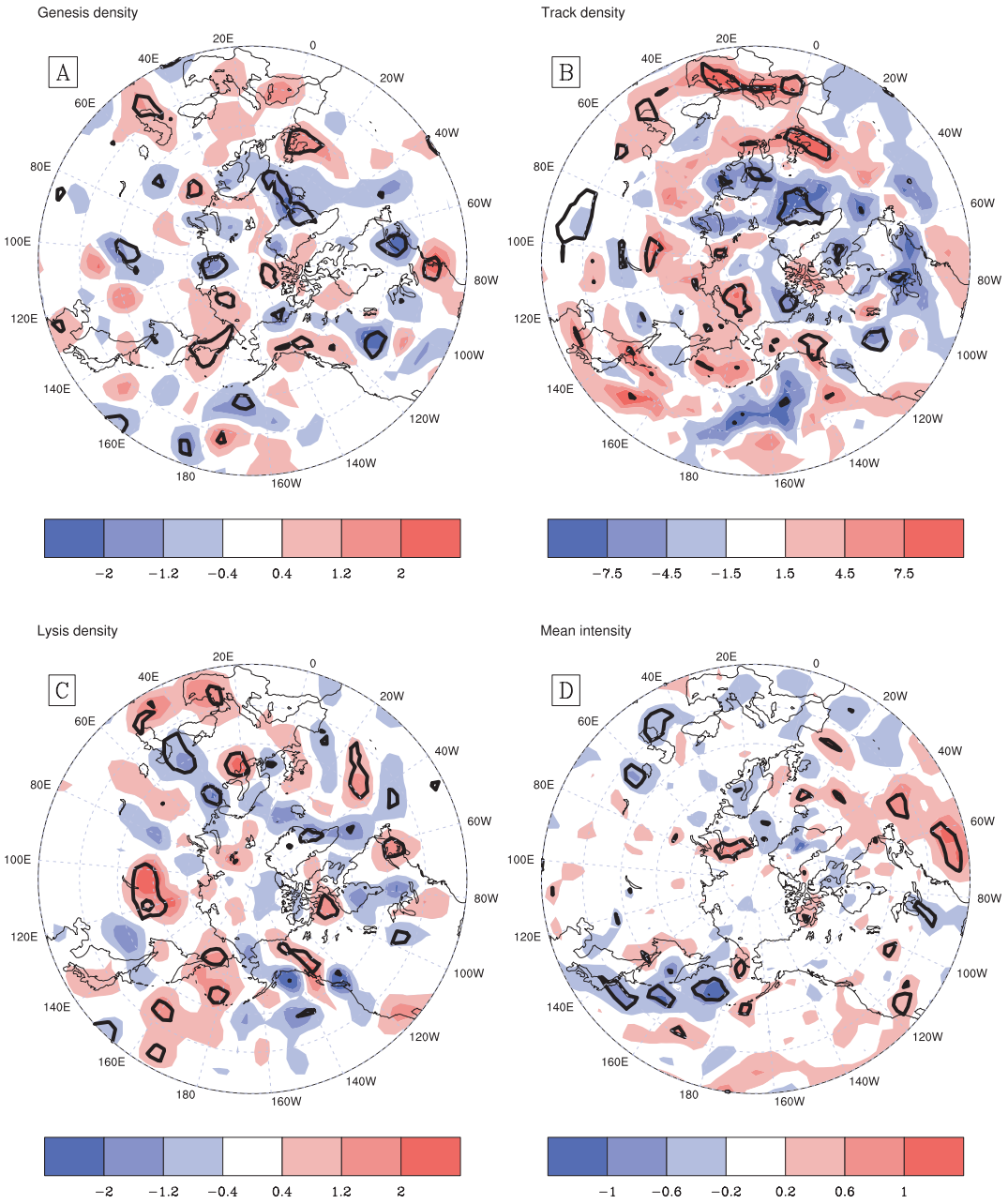

Fig. 2. 850 hPa storm track composites for SOKc+ minus SOKc– (1978(9)–2007): (a) genesis density, density of track starting points per $(10^6$ km^2 season$)^{-1}$; (b) track density, number of storm tracks through a region per $(10^6$ km^2 season$)^{-1}$; (c) lysis density, density of ending track points per $(10^6$ km^2 season$)^{-1}$; (d) mean track intensity, mean strength of the vortices in units of 10^{-5} s^{-1}. The thick black lines indicate regions where the *p*-values are less than 5% (see Hodges, 2008 for the significance estimation).

km^2 season$)^{-1}$ and (4) mean intensity (*mint*)—mean strength of the vortices in units of 10^{-5} s^{-1}. Here, we will focus mainly on the Pacific and Atlantic changes.

3.2.1 Genesis density. The *gdens* plot (Fig. 2a) shows more storms being formed in parts of the Bering Sea, Kamchatka and southern Alaska when SOKc is positive, consistent with Overland and Pease (1982). They could represent generation of storms due to local baroclinicity, since higher sea ice in the SOK could lead to higher north–south gradient of temperature in the Kamchatka area. In the Atlantic, more storms are observed to generate over the western approaches of the United Kingdom, these are also most likely due to secondary generation. More storms are also seen to generate east of the United States.

Reduced genesis is found over the SOK, indicating that more sea ice in that region helps to cut off the sensible heat source for storms to be generated there. Another striking feature is the reduction in the storms over the main track in the Pacific, the region of *secondary cyclogenesis* (Hoskins and Hodges, 2002; Mesquita et al., 2010). The *gdens* decrease in the Atlantic is mostly along the east coast of North America (Nova Scotia) and through the Icelandic region towards Scandinavia. The reduction over Nova Scotia is mirrored by an increase further south over Cape Hatteras, which together with the increased secondary cyclogenesis downstream may indicate a more southerly storm track. The Atlantic results have some similarity with a negative NAO phase.

3.2.2. Track density. The *tdens* plot (Fig. 2b) shows results that reflect the differences in *gdens*, except that they are not as significant. The suppression of storms in the mid-Pacific towards the Gulf of Alaska looks like an equatorward shift at the end of the Pacific storm track. Hence, the changes to the downstream development of storm tracks (Honda et al., 1999) could be related to the shift mentioned, but since only a few areas are significant, the overall impact there is low. The most significant impact in the Pacific is over the Yukon region.

In the Atlantic region, there seems to be an equatorward shift in the storm track with more storms into the United Kingdom and through the Mediterranean (similar to a negative phase of the NAO). These negative-NAO-like features could be related to the NAO damping due to changes in the sea-ice concentration over the SOK, as suggested by Yamamoto et al. (2006). The authors showed that changes in the North Pacific and North America are linked to changes in the SOK sea-ice variability through the formation of a stationary Rossby wave train. They also suggested that a positive phase of the Northern Hemisphere ice seesaw (sea-ice variability pattern with one polarity in the Bering and Labrador Seas and the other in the Okhotsk and Greenland-Barents Seas)—dominant in mid-winter—appears as a response to a positive NAO and anticyclonic anomalies over the North Pacific in early winter. In turn, the mid-winter positive sea-ice seesaw damps the positive NAO signal. In late winter, a negative phase of the NAO is observed—damped by the sea-ice seesaw in the North Pacific: reflected as a stationary Rossby wave excited over the SOK. A more detailed analysis of the relationship between the SOK sea-ice changes and the NAO will be addressed in a separate paper.

3.2.3. Lysis density. A striking difference is seen in the *ldens* plot (Fig. 2c) in the Pacific. The west Pacific shows more storms dying there when SOKc is positive. It is important to emphasize that SOKc could also be a response to cold temperatures and sea-ice conditions over Eurasia and Siberia, which could also be affecting the North Pacific (Orsolini and Kvamstø, 2009). The SOK is also exposed to the cold air-pressure system of the Siberian high and the Aleutian low—where the position and intensity of the Aleutian low may largely determine the advance or retreat of sea-ice in the SOK (Rikiishi and Takatsuji, 2005). Hence, cold temperatures as seen in the positive phase of SOKc could suppress the storm tracks, making them die earlier, before reaching the Gulf of Alaska ('GOA' hereafter). GOA is known to be the region where most storms die in the North Pacific (Hoskins and Hodges, 2002; Simmonds and Keay, 2002) and trends over GOA are not explained by the local changes of SST (Mesquita et al., 2010). For positive SOKc, storms die before reaching GOA: either in the west Pacific or over the Aleutians. Storms that are generated over the Aleutians/Bering Sea end up dying over the Yukon/British Columbia area.

In the Atlantic, we see a coherent pattern in the *ldens* case: storms die more frequently over the United Kingdom and central Europe and less in the region between southern Greenland, Scandinavia and eastern Europe—very similar to a negative NAO-like pattern.

3.2.4. Mean intensity. The mean intensity (Fig. 2d) pattern shows reduced storm track intensity over and south of the Kamchatka area and on a large area of the west Pacific Ocean. These are regions of intense systems in the winter season (Mesquita et al., 2010). More intense systems are also found close to the Bering Strait and over the Aleutians. In the Atlantic, a shift in the pattern is observed: in this case, more intense systems in the south and less intense in the North.

3.3. Seeding

One mechanism in which the observed changes in the Atlantic (southward shift of the storms) could be explained is through the idea of 'seeding' (Chang et al., 2002; Hoskins and Hodges, 2002): at higher levels, storms (in the form of upper level troughs) travel long distances and they may seed other storms, that is, they may provide the background for new storm development and growth in the Atlantic sector. This is the case of the Pacific storms seeding storms in the Atlantic. Pacific and Atlantic storm track variations are correlated—a stronger Pacific storm track could lead to a stronger Atlantic storm track (Chang and Fu, 2002).

Figure 3 shows the storms tracked at the 250 hPa level. There are more storms over the Atlantic during positive phases of the SOKc—possibly indicating more seeding, through the Pacific storms. The Atlantic southward shift of 250 hPa storm tracks are clearly seen for the genesis and track density variables—this also points to an equivalent barotropic response in the Atlantic. The southward shift also leads to an overall decrease in the intensity of storms in the northern North Atlantic.

The seeding could very well change the eddy-driven jet. A significant change in the downstream part of the Atlantic and over the subtropical jet region is observed in February (not shown), which suggests that the polar jet is more southerly.

3.4. Is it a seasonal feature?

The sea-ice changes in the SOK may have some impact on storm tracks, especially in the Atlantic region. However, the sea-ice

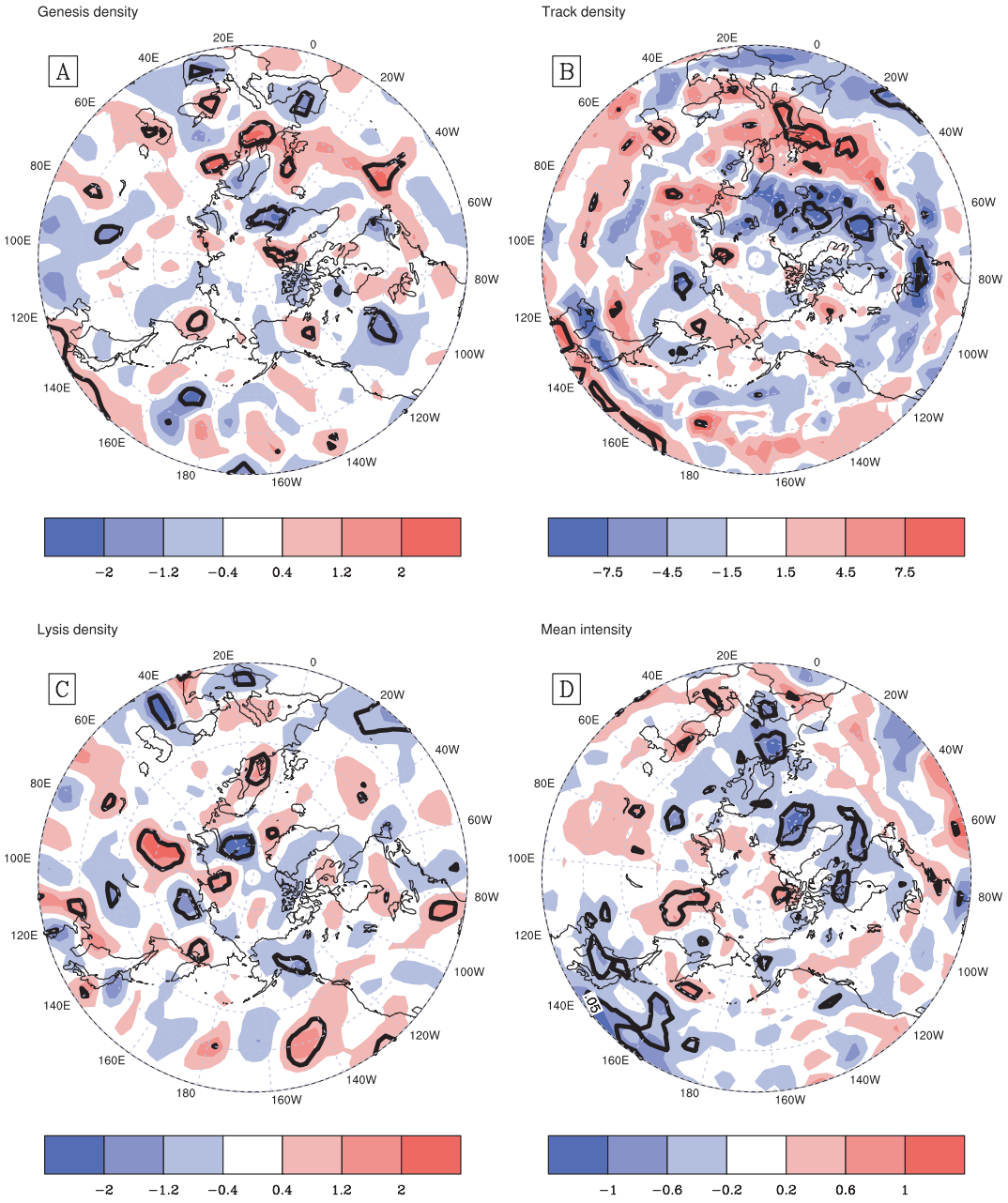

Fig. 3. 250 hPa storm track composites for SOKc+ minus SOKc– (1978(9)–2007): (a) genesis density, density of track starting points per (10^6 km^2 season)$^{-1}$; (b) track density, number of storm tracks through a region per (10^6 km^2 season)$^{-1}$; (c) lysis density, density of ending track points per (10^6 km^2 season)$^{-1}$; (d) mean track intensity, mean strength of the vortices in units of 10^{-5} s^{-1}. The thick black lines indicate regions where the *p*-values are less than 5% (see Hodges, 2008 for the significance estimation).

concentration in December is much lower and less variable than that at the end of the season. In late winter, such changes may point to a higher variability in storm tracks due to either heavy or light sea-ice conditions. This is especially true when considering the highest variability months (January and February), as confirmed by the changes in geopotential height (Fig. 4). The figure shows 500 hPa geopotential height for January and February regressed onto the sea-ice concentration in the SOK. The pattern is different, especially in the Atlantic, when December is considered alone or included in the regression.

In order to further investigate this relationship, we selected 5 months with highest sea-ice concentration values and 5 with the least sea-ice. Other authors have also done compositing in a similar fashion: Deser et al. (2000), who selected years based on the standard deviation; Johnson (1980), who selected five Januaries of maximum sea ice and five Januaries with minimum

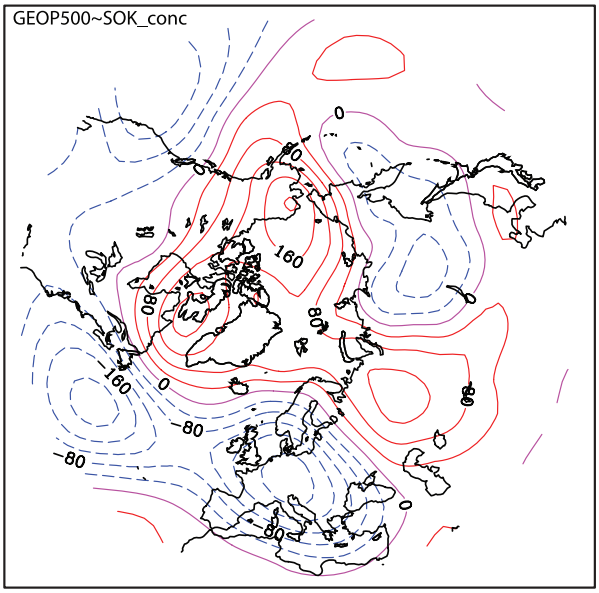

Fig. 4. Monthly 500 hPa geopotential height regressed against the SOK concentration for January and February (in m). Blue, red and magenta lines represent negative, positive and zero values, respectively.

sea ice in the Arctic; and Honda et al. (1999), who selected five heavy and light sea-ice years in the SOK for the numerical integrations and four heaviest and lightest sea-ice years in the SOK for the observations.

Figures 5a and b show our composites for the 1000 hPa and the 500 hPa levels, respectively. The selected months with highest sea ice correspond mostly to February (1979, 1980, 1983 and 2001) with the exception of January 1979. The selected months with the lowest sea-ice concentration correspond to December (1988, 1995, 1997, 1999 and 2005). The response shows a negative NAO-like pattern. We may not rule out the El Niño Southern Oscillation effect in the composite plot, which could explain the greater variability there. However, the patterns observed indicate that the sea-ice conditions in the SOK in later winter may provide an impact.

We have also tracked storms in the 850 hPa relative vorticity data corresponding to the five highest and lowest sea-ice concentration data. The compositing difference is shown in Fig. 5c (See Hodges, 2008 for a description of the significance calculation). The overall results in the Atlantic show a decrease in the number of storms in the northern part of the Atlantic, especially over Scandinavia—again pointing to a negative NAO-like pattern. In the Pacific, we see an increase in the number of storms. This could be a local effect due to the temperature gradient between the cold continent and warm ocean. Honda et al. (1999) also found a sea level pressure decrease over that area in their 'five-heavy-and-five-light' composites. There is also an increase in the number of storms in the downstream part of the Pacific storm track. This could indicate that changes to the downstream development, due to sea-ice changes in the SOK (Honda et al., 1999), are mostly significant in late winter.

The changes observed here could as well be casual. However, in order to isolate the SOK influence, we have conducted experiments using the ECHAM5 model, as outlined below.

3.5. *ECHAM5 simulations*

Two sets of simulations were conducted in an attempt to understand the influence of the SOK sea ice on the atmospheric circulation. Figure 6a shows the area where the sea ice was changed (full sea-ice and no sea-ice simulations). Figure 6b shows the corresponding sensible plus the latent heat anomalies in the SOK region.

Figures 7a and b show the response (full sea-ice minus no sea-ice) in DJF geopotential in 500 hPa and 1000 hPa. The comparison between the simulated (Figs 7a and b) and observed (Figs 4 and 5a,b) geopotential height patterns show differences, especially in the Pacific sector. To first order, the simulated response in Figs 7a and b show a direct, linear baroclinic response to the surface cooling. It features a surface high (Fig. 7a) in the SOK with an upper level low (Fig. 7b) above. The observed pattern is markedly different from the simulated pattern in the Pacific region, especially over the SOK region. In order to find out the reason for the difference between the observed and simulated patterns in the Pacific region we have tested the robustness of the observed pattern. This has been done because of the small observed sample size. In contrast to the simulation (30 ensemble members for each experiment), we only have five observational members for each (high and low) SOK sea-ice condition. Therefore, we varied the composite using different criteria. For example, we applied the criterion used by Honda et al. (1999) to define the composite. Honda et al.'s criterion uses only four heaviest and lightest February SOK anomalies for the observations. Although using an extended data set compared to Honda et al. (1999), the pattern was almost the same as figure 13a in Honda et al. (1999)—showing more agreement with our simulated geopotential height anomaly pattern.

From our analysis, it turned out that the response in the Pacific sector strongly depends on the composite criteria chosen: the observational pattern in the Pacific seems not to be robust. In contrast, the observational geopotential height anomaly pattern in the Atlantic (negative NAO-like pattern) was robust for all composites. The simulated geopotential height patterns (Figs 7a and b) in the Atlantic region show a significant NAO-like pattern. The response appears to be equivalent barotropic in the Atlantic. A dipole-like structure is also evident in the reanalysis data (Figs 4 and 5a and b). The similarity of the geopotential height anomaly patterns (NAO-like pattern) between the simulated (causal/physical link) and observed (statistical link) supports the hypothesis that the NAO-like pattern in the Atlantic region is forced by the SOK sea-ice anomalies.

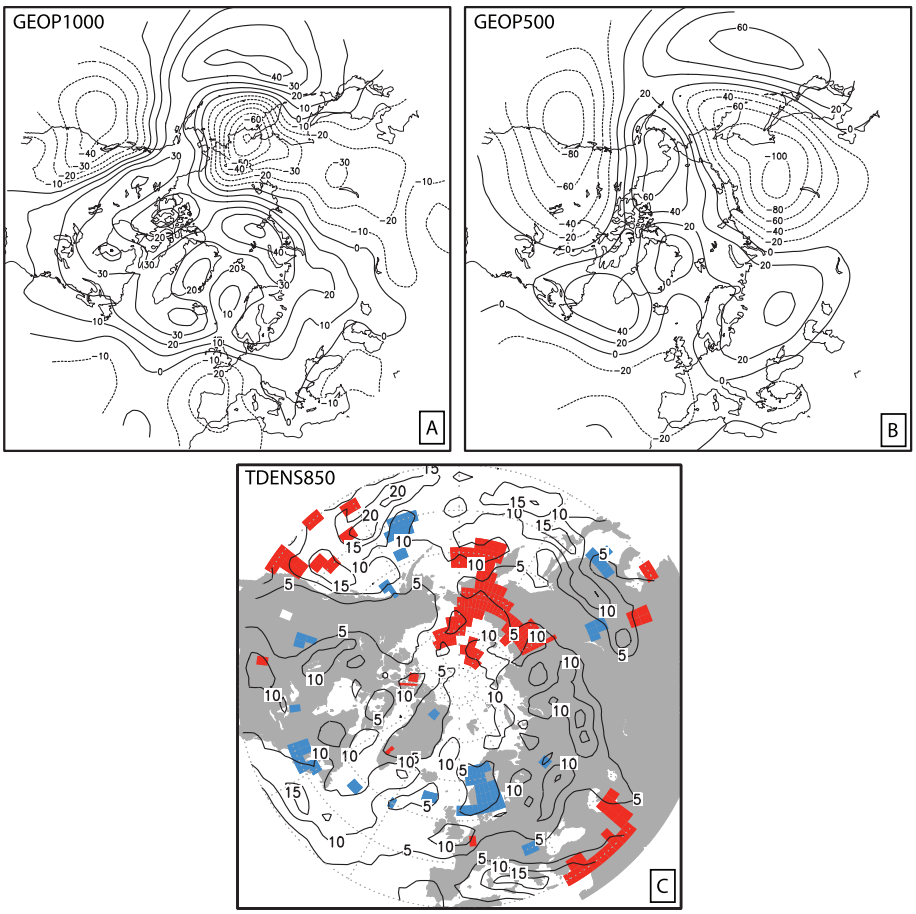

Fig. 5. (a) Observed 1000 hPa geopotential height difference of the composite of the five highest (positive) minus the five lowest (lowest) SOK sea-ice concentration values; between the positive and negative values, Unit: gpm; (b) same as A, but for the 500 hPa level; (c) contours represent the observed 850 hPa track density for the five highest SOK sea-ice concentration values (climatology of the positive composite). Colours represent the track density difference of the composite. Only areas statistically significant at the 95% level are coloured. Red/blue represents significant enhancement/reduction of the track density. Unit: number of storm tracks through a region per $(10^6$ km^2 season$)^{-1}$.

The NAO-like response in the Atlantic is also shown in the track density difference between the ECHAM5 full sea-ice simulation minus the no sea-ice one, as shown in Fig. 8. The contours in Fig. 8 show the DJF 850 hPa track density for the full SOK sea-ice experiment. The colours represent significant changes of the DJF track density between the full and no sea-ice SOK experiments. Red/blue colouring indicates significant enhancement/reduction of the track density between the two experiments (full minus no SOK sea-ice runs). There is a clear dipole-like pattern in the Atlantic—significant reductions in the northern mid-latitudes and significant enhancement of the storm track in the subtropical region. The observed changes in the track density (Fig. 5c) associated with the five highest minus the five lowest sea-ice concentrations in the SOK features also a dipole-like structure in the Atlantic sector, but only with significant reductions in the northern mid-latitudes and Scandinavia. The Atlantic dipole-like pattern in the storm track density is confirmed in Figs 2b (DJF 850 hPa track density composite) and 3b (DJF 250 hPa track density composite). A closer look reveals that the dipole-like pattern in Figs 2b and 3b are more pronounced than that in Fig. 5c. This might be due to the fact that the data size used for Figs 2b and 3b is much larger—the whole winter season (DJF) was used.

In summary, a dipole-like structure in the Atlantic sector is evident in the mean geopotential height anomaly pattern and in the storm track density—both in the observations and in the simulations. There is a disagreement in the geopotential height anomaly pattern between the reanalysis data and the simulations in the Pacific sector. In light of these findings, how can changes in the Pacific force the Atlantic changes?

Chang and Fu (2002) show that the Pacific and Atlantic storm track variations are correlated. They mention two possible mechanisms between the dynamical link of the two storm tracks. 'One possibility could arise from the fact that the eddies in the Atlantic storm track are seeded by the Pacific storm track (see Chang and Yu, 1999). A stronger Pacific storm track could

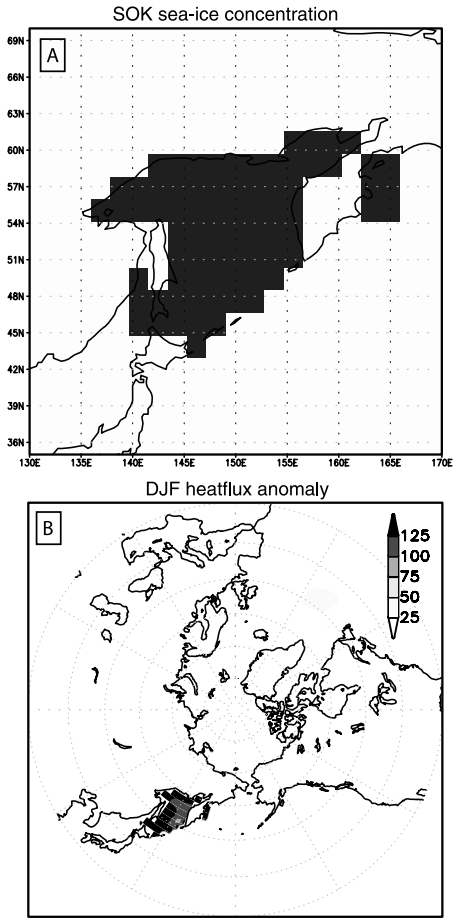

Fig. 6. (a) Area where the SOK sea ice is set to zero or 100% in the ECHAM5 simulations. The ECHAM5 negative experiment used no sea-ice; (b) the sensible plus the latent heat flux anomalies of the 0% SIC minus 100% SIC for the DJF (December, January and February) season. Units in: W m^{-2}. Only positive values are shown. Positive means from the ocean to the atmosphere.

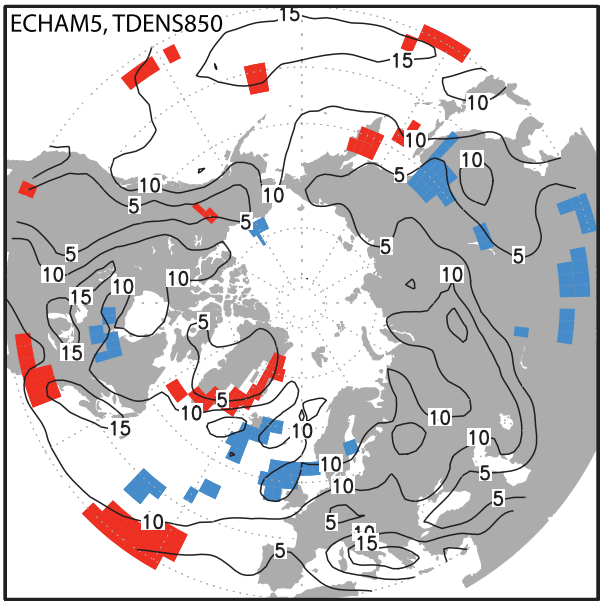

Fig. 8. DJF track density difference between the ECHAM5 simulations with a full sea-ice cover in the Sea of Okhotsk (SOK) and no sea ice in the region. Contours represent the 850 hPa track density of the full sea-ice experiment. Colours represent the track density difference between the full sea-ice and no sea-ice (in the SOK) experiments. Only areas statistically significant at the 95% level are coloured. Red/blue represents significant enhancement/reduction of the track density. Unit: number of storm tracks through a region per (10^6 km^2 season)$^{-1}$.

conceivably lead to a stronger Atlantic storm track'. Alternatively, one could imagine that 'the correlation between the two basins arise from the low-frequency flow rather than due to the effect of the synoptic scale eddy propagation and seeding' (Chang and Fu, 2002, p. 651).

In our case, since the Pacific mean observational pattern is not robust, we believe that the interaction is taking place via

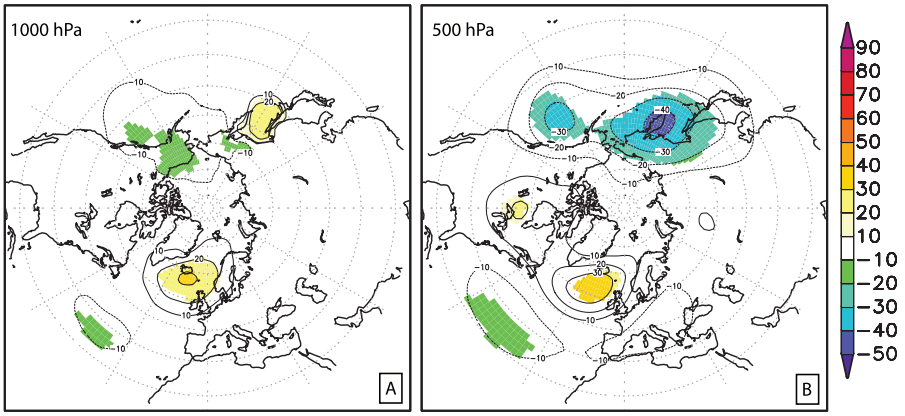

Fig. 7. Geopotential height response between the ECHAM5 runs with a full sea-ice cover in the Sea of Okhotsk (SOK) and no sea ice in that region. The contours show the simulated mean winter (DJF) geopotential height response in (a) 1000 hPa and (b) 500 hPa; and (c) the February 300 hPa eddy geopotential height response. Areas statistically significant at the 95% level are coloured. Unit: gpm.

seeding of the storms (see our Section 3.3 on seeding): much of the atmospheric variability is associated with upstream seeding (Orlanski, 2005) and an important issue determining the NAO phase is related to upstream effects (Rivière and Orlanski, 2007). Even single storm events may be enough to trigger changes in the phase of the NAO index (Rivière and Orlanski, 2007). Positive and negative phases of the NAO are also closely related to anticyclonic and cyclonic Rossby wave breaking, respectively. The studies of Riviere and Orlanski (2007) and Strong and Magnusdottir (2008a,b) indicate that Rossby wave breaking over the Pacific are important for determining the NAO phase. A detailed statistical analysis of wave breaking in our experiments is subject of a new manuscript and it is beyond the scope of this study.

The ECHAM5 simulations confirm our observational-based result that sea-ice changes in the SOK have a significant impact on the atmospheric circulation and on the storm tracks in the Atlantic sector.

4. Conclusion

This paper has discussed the relationship between the sea-ice changes in the SOK and the extratropical storm tracks in the Northern Hemisphere. There are different mechanisms at play in that region: First, sea-ice cover over the SOK is influenced by changes in the storm tracks associated with the large-scale circulation (Fang and Wallace, 1994; Honda et al., 1999), the physical implications of which can operate in both directions (Honda et al., 1999). Second, sea-ice variability anomalies are also associated with anomalies in pressure patterns [e.g. the Aleutian low and Siberian high (Honda et al., 2001)]. This is especially the case for the position and intensity of the Aleutian low (Rikiishi and Takatsuji, 2005), whereas the correspondence between the SOK sea-ice extent and the Siberian high is not maintained throughout the whole period of the observational record (Parkinson, 1990). Finally, the presence of sea ice reduces heat and moisture fluxes from the sea surface—cooling the air above (Honda et al., 1999).

Overall, our study shows that the sea-ice cover over the SOK may affect most storm track variables, not only in the North Pacific, but also in the Atlantic. Our results have shown that:

(1) The SOK sea-ice variability plays a significant role in the storm track changes. The influence is larger in the Atlantic sector;

(2) Changes in the SOK sea ice could also help explain some of the trend variability in the GOA region (e.g. track density and intensity). If local SSTs are not influencing GOA (Mesquita et al., 2010), then a plausible explanation would be that the large-scale atmospheric variability and changes on the sea-ice cover in the SOK could be at play.

(3) The decrease in secondary cyclogenesis, increase in lysis density and decrease of mean intensity in the Pacific sector provide an important contribution to changes in the seeding of storms in the Atlantic. Fewer storms in the northern sector of the Atlantic are seeded. And these changes alter the eddy driven jet in the Atlantic as well, making it more southerly.

(4) The seeding from the Pacific storms into the Atlantic help change the Atlantic eddy-driven jet, thus altering the transient eddy vorticity fluxes (as shown by Franzke and Feldstein, 2005, most low-frequency patterns in the North Atlantic are driven by transient eddy vorticity fluxes)—and it is the low-frequency vorticity flux and divergence that could contribute to the changes in the Atlantic.

(5) The SOK sea-ice variability in late winter plays a more important role—the time when the sea-ice changes are higher.

(6) The sensitivity experiment with no sea-ice in the SOK show a negative NAO-like response, in agreement with the observed changes in late winter.

(7) The changes of downstream development due to sea-ice changes in the SOK (Honda et al., 1999) are mainly important in late winter. The overall winter (DJF) storm track climatology shows changes mostly in the upstream and mid-storm track development.

In future work, we plan to also include longer data sets and to incorporate data from newer high-resolution reanalyses, for example, ERA-Interim, NASA-MERRA or NCEP-CFS.

5. Acknowledgments

We are grateful for NCAR and NSIDC for providing their data sets in the public domain. We thank the Max-Planck-Institute for Meteorology for providing and supporting the ECHAMS model. We also thank Drs. Uma Bhatt, Xiangdong Zhang and John Walsh for the helpful comments on an earlier version of the manuscript, as well as the anonymous reviewers and the Tellus A editor, Dr. Harald Lejenäs. We would also like to thank the University of Alaska Fairbanks, the International Arctic Research Center, the University of Reading and the Bjerknes Centre for Climate Research for the computational and other resources provided during this study. The graphics were produced with the GrADS software package developed by Brian Doty, and the NCAR Command Language. This work was made possible by the NOAA Grant NA06OAR4600179 'Social Vulnerability to Climate Change in the Alaskan Coastal Zone'. JB's work was supported by the DecCen and the COMPAS projects funded by the Research Council of Norway. The model runs have been performed at the Norwegian Metacenter for Computational Science (NOTUR). This is publication no. A299 from the Bjerknes Centre for Climate Research.

References

Alexander, M. A., Bhatt, U. S., Walsh, J. E., Timlin, M. S., Miller, J. S. and co-authors. 2004. The atmospheric response to realistic arctic sea ice anomalies in an AGCM during winter. *J. Clim.* **17**, 890–905.

Bengtsson, L., Hodges, K. I. and Roeckner, E. 2006. Storm tracks and climate change. *J. Clim.* **19**, 3518–3543.

Cavalieri, D., Parkinson, C., Gloersen, P. and Zwally, H. J. 2008. Sea ice concentrations from Nimbus-7 SMMR and DMSP SSM/I passive microwave data. Accessed: 29 June 2009. Boulder, Colorado, USA : National Snow and Ice Data Center. Digital media.

Chang, E. K. M. and Fu, Y. 2002. Interdecadal variations in Northern Hemisphere winter storm track intensity. *J. Clim.* **15**, 642–658.

Chang, E. K. M. and Yu, D. B. 1999. Characteristics of wave packets in the upper troposphere. Part I: Northern Hemisphere winter. *J. Atmos. Sci.* **56**, 1708–1728.

Chang, E. K. M., Lee, S. and Swanson, K. L. 2002. Storm track dynamics. *J. Clim.*, **15**, 2163–2183.

Deser, C., Walsh, J. E. and Timlin, M. S. 2000. Arctic Sea ice variability in the context of recent atmospheric circulation trends. *J. Clim.* **13**, 617–633.

Deser, C., Magnusdottir, G., Saravanan, R. and Phillips, A. 2004. The effects of north Atlantic SST and sea ice anomalies on the winter circulation in CCM3. Part II: direct and indirect components of the response. *J. Clim.* **17**, 877–889.

Fang, Z. and Wallace, J. M. 1994. Arctic sea ice variability on a timescale of weeks and its relation to atmospheric forcing. *J. Clim.* **7**, 1897–1914.

Franzke, C. and Feldstein, S. B. 2005. The continuum and dynamics of Northern Hemisphere teleconnections patterns. *J. Atmos. Sci.* **62**, 3250–3267.

Hodges, K. I. 1994. A general method for tracking analysis and its application to meteorological data. *Mon. Weather Rev.* **122**, 2573–2586.

Hodges, K. I. 1995. Feature tracking on the unit sphere. *Mon. Weather Rev.* **123**, 3458–3465.

Hodges, K. I. 1996. Spherical nonparametric estimators applied to the UGAMP model integration for AMIP. *Mon. Weather Rev.* **124**, 2914–2932.

Hodges, K. I. 1999. Adaptive constraints for feature tracking. *Mon. Weather Rev.* **127**, 1362–1373.

Hodges, K. I., Hoskins, B. J., Boyle, J. and Thorncroft, C. 2003. A comparison of recent re-analysis data sets using objective feature tracking: storm tracks and tropical easterly waves. *Mon. Weather Rev.* **131**, 2012–2037.

Hodges, K. I. 2008. Confidence intervals and significance tests for spherical data derived from feature tracking. *Mon. Weather Rev.* **136**, 1758–1777.

Honda, M., Nakamura, H., Ukita, J., Kousaka, I. and Takeuchi, K. 2001. Interannual seesaw between the Aleutian and Icelandic lows. Part I: seasonal dependence and life cycle. *J. Clim.* **14**, 1029–1042.

Honda, M., Yamazaki, K., Nakamura, H. and Takeuchi, K. 1999. Dynamic and thermodynamic characteristics of atmospheric response to anomalous sea-ice extent in the Sea of Okhotsk. *J. Clim.* **12**, 3347–3358.

Hoskins, B. J. and Hodges, K. I. 2002. New perspectives on the Northern Hemisphere winter storm tracks. *J. Atmos. Sci.* **59**, 1041–1061.

Johnson, C. M. 1980. Wintertime Arctic Sea ice extremes and the simultaneous atmospheric circulation. *Mon. Weather Rev.* **108**, 1782–1791.

Kalnay, E., Kanamitsu, M., Kistler, R., Collins, W., Deaven, D., and co-authors. 1996. The NCEP-NCAR 40-year reanalysis project. *Bull. Am. Meteorol. Soc.* **77**, 437–471.

Kistler, R., Kalnay, E., Collins, W., Saha, S., White, G. and co-authors. 2001. The NCEP-NCAR 50-year reanalysis: monthly means CD-ROM and documentation. *Bull. Am. Meteorol. Soc.* **82**, 247–267.

Magnusdottir, G., Deser, C. and Saravanan, R. 2004. The effects of north Atlantic SST and sea ice anomalies on the winter circulation in CCM3. Part I: main features and storm track characteristics of the response. *J. Clim.* **17**, 857–876.

Mesquita, M. d. S., Atkinson, D. E. and Hodges, K. I. 2010. Characteristics and variability of storm tracks in the North Pacific, Bering Sea and Alaska. *J. Clim.* **23**, 294–311.

Murray, R. J. and Simmonds, I. 1995. Responses of climate and cyclones to reductions in Arctic winter sea ice. *J. Geophys. Res.* **100**, 4791–4806.

Orlanski, I. 2005. A new look at the Pacific storm track variability: sensitivity to tropical SSTs and to upstream seeding. *J. Atmos. Sci.* **62**, 1367–1390.

Orsolini, Y. J. and Kvamstø, N. G. 2009. The role of the Eurasian snow cover upon the wintertime circulation: decadal simulations forced with satellite observations. *J. Geophys. Res.* **114**, D19108. doi:10.1029/2009JD012253.

Overland, J. E. and Pease, C. H. 1982. Cyclone Climatology of the Bering Sea and Its Relation to Sea Ice Extent. *Mon. Weather Rev.* **110**, 5–13.

Parkinson, C. L. 1990. The impact of the Siberian high and Aleutian low on the sea-ice cover of the Sea of Okhotsk. *Ann. Glaciol.* **14**, 226–229.

Partington, K., Flynn, T., Lamb, D., Bertoia, C. and Dedrick, K. 2003. Late twentieth century Northern Hemisphere sea-ice record from U.S. National Ice Center ice charts. *J. Geophys. Res.* **108**, 3343. doi:3310.1029/2002JC001623.

Rikiishi, K. and Takatsuji, S. 2005. On the growth of ice cover in the Sea of Okhotsk with special reference to its négative corrélation with that in the Bering Sea. *Ann. Glaciol.* **42**, 380–388.

Rivière, G. and Orlanski, I. 2007. Characteristics of the Atlantic storm-track eddy activity and its relation with the North Atlantic oscillation. *J. Atmos. Sci.* **64**, 241–266.

Roeckner, E., Bäuml, G., Bonaventura, L., Brokopf, R., Esch, M. and co-authors. 2003. The atmospheric general circulation model ECHAM 5. In MPI Report 349.

Roeckner, E., Brokopf, R., Esch, M., Giorgetta, M., Hagemann, S. and co-authors. 2006. Sensitivity of simulated climate to horizontal and vertical resolution in the ECHAM5 atmosphere model. *J. Clim.* **19**, 3771–3791.

Rogers, J. C. and van Loon, H. 1979. The seesaw in winter temperatures between Greenland and Northern Europe. Part II: some oceanic and atmospheric effects in middle and high latitudes. *Mon. Weather Rev.* **107**, 509–519.

Seierstad, I. A. and Bader, J. 2009. Impact of a projected future Arctic sea ice reduction on extratropical storminess and the NAO. *Clim. Dyn.* **33**, 937–943, doi:10.1007/s00382-008-0431-5.

Simmonds, I. and Budd, W. F. 1991. Sensitivity of the sourthern hemisphere circulation to leads in the Antarctic pack ice. *Quart. J. Roy. Meteor. Soc.* **117**, 1003–1024.

Simmonds, I. and Keay, K. 2002. Surface fluxes of momentum and mechanical energy over the north Pacific and north Atlantic oceans. *Meteor. Atmos. Phys.* **80**, 1–18.

Strong, C. and Magnusdottir, G. 2008a. Tropospheric Rossby wave breaking and the NAO/NAM. *J. Atmos. Sci.* **65**, 2861–2876.

Strong, C. and Magnusdottir, G. 2008b. How Rossby wave breaking over the Pacific forces the North Atlantic oscillation. *Geophys. Res. Lett.* **35**, L10706. doi:10.1029/2008GL033578.

Toyota, T., Ukita, J., Ohshima, K. I., Wakatsuchi, M. and Muramoto, K. 1999. A measurement of sea ice albedo over the southwestern Okhotsk Sea. *J. Meteorol. Soc. Jpn.* **77**, 117–133.

Woollings, T., Hoskins, B., Blackburn, M., Hassell, D. and Hodges, K. I. 2010. Storm track sensitivity to sea surface temperature resolution in a regional atmosphere model. *Clim. Dyn.* **35**, 341–353.

Yamamoto, K., Tachibana, Y., Honda, M. and Ukita, J. 2006. Intraseasonal relationship between the Northern Hemisphere sea ice variability and the North Atlantic oscillation. *Geophys. Res. Lett.* **33**, L14711, doi:10.1029/2006GL026286.